Computers and Electronics in Agriculture 148 (2018) 280–290

Contents lists available at ScienceDirect

Computers and Electronics in Agriculture

journal homepage: www.elsevier.com/locate/compag

Original papers

A knowledge-and-data-driven modeling approach for simulating plant growth and the dynamics of CO_2/O_2 concentrations in a closed system of plants and humans by integrating mechanistic and empirical models

Xing-Rong Fan[a,b], Xiujuan Wang[b,f], Mengzhen Kang[b,c,*], Jing Hua[b,c], Shuangsheng Guo[d,*], Philippe de Reffye[e], Bao-Gang Hu[f]

[a] Electronic Information and Networking Research Institute, Chongqing University of Posts and Telecommunications, Chongqing 400065, China
[b] The State Key Laboratory of Management and Control for Complex Systems, Institute of Automation, Chinese Academy of Sciences, Beijing 100190, China
[c] Qingdao Academy of Intelligent Industries, Qingdao 266109, China
[d] National Key Laboratory of Human Factors Engineering, China Astronaut Research and Training Center, Beijing 100094, China
[e] Cirad-Amis, UMR AMAP, TA 4001 Avenue Agropolis, F-34398 Montpellier, Cedex 5, France
[f] National Laboratory of Pattern Recognition, Institute of Automation, Chinese Academy of Sciences, Beijing 100190, China
[f] Beijing Engineering Research Center of Intelligent Systems and Technology, Beijing, 100190, China

ARTICLE INFO

Keywords:
Closed ecological life support system
Functional-structural plant model
Knowledge-and-data-driven model
Mass balance model
Model evaluation
And model verification

ABSTRACT

Modeling and the prediction of material flows (plant production, CO_2/O_2 concentrations, H_2O) is an important but challenging task in the design and control of closed ecological life support systems (CELSS). The aim of this study was to develop a novel knowledge-and-data-driven modeling (KDDM) approach for simultaneously simulating plant production and CO_2/O_2 concentrations in a closed system of plants and humans by integrating mechanistic and empirical models.

The KDDM approach consists of a 'knowledge-driven (KD)' sub-model and a 'data-driven (DD)' sub-model. The KD sub-model describes hourly and up to daily plant photosynthesis, respiration and assimilation partitioning using the components of GreenLab and TomSim models. The DD sub-model describes the dynamics of CO_2 production and O_2 consumption by the crew member using a piecewise linear model. The two sub-models were integrated with a mass balance model for CO_2/O_2 concentrations in a closed system.

The KDDM was applied with a two-person, 30-day integrated CELSS test. This model provides accurate computation of both the dry weights of different plant compartments and CO_2/O_2 concentrations. The model also quantifies the underlying material flows among the crew members, plants and environment.

This approach provides a computational basis for lifetime optimization of cabin design and experimental setup of CELSS (*e.g.*, environmental control, planting schedule). With extension, this methodology can be applied to a half-closed system such as a glasshouse.

1. Introduction

Closed Ecological Life Support Systems (CELSS) are self-supporting life support systems for space stations and colonies, typically using controlled closed ecological systems. To date, CELSS have been widely acknowledged as playing a vital role in future regenerative life support systems for long-term human deep space exploration, space technology development, and space colonization (Guo et al., 2014a; Wheeler and Sager, 2006). These systems can provide basic life-support requirements for crew members, such as food, oxygen and drinking water, using plants as the central recycling component. Therefore, research programs on CELSS have been implemented at the national space agencies and universities, such as the University of Arizona (Biosphere 2, USA), the Institute of Biophysics in Krasnoyarsk (BIOS-3, Russia), Beijing University of Aeronautics and Astronautics (Yuegong-1, China), and the European Space Agency (MELiSSA). One of the most important elements of CELSS is the growth of higher plants in a controlled environment for the production of food and oxygen (O_2) from 'waste' carbon dioxide (CO_2) (Finetto et al., 2008; Guo et al., 2008; Hezard et al., 2012;Wheeler, 2015).

Since the experiments of CELSS are high-cost and time-consuming, a mass-balance model for life support systems needs to be developed in at

* Corresponding authors at: The State Key Laboratory of Management and Control for Complex Systems, Institute of Automation, Chinese Academy of Sciences, Beijing 100190, China (M.Z. Kang), and National Key Laboratory of Human Factors Engineering, China Astronaut Research and Training Center, Beijing 100094, China (S.S. Guo).
E-mail addresses: mengzhen.kang@ia.ac.cn (M. Kang), guoshuangsheng@sina.com (S. Guo).

https://doi.org/10.1016/j.compag.2018.03.006
Received 23 May 2017; Received in revised form 28 February 2018; Accepted 4 March 2018
Available online 30 March 2018
0168-1699/

least two dimensions: firstly, it must predict important fluxes (*e.g.*, edible biomass, CO_2/O_2 concentrations), and secondly, it must provide environmental control of the plant and human compartments. As plants are complex and dynamic systems, their growth and development involves a large number of interconnected ecophysiological processes. Significant progress has been reported in studies of modeling, simulation and visualization of plant growth in recent decades (Diao et al., 2012; de Reffye and Hu, 2003; Fan et al., 2015; Vos et al., 2009; Yin and Struik, 2016). Early process-based models (PBMs) consider the environment as the main variable driving plant growth and focus on plant functioning in relation to environmental conditions, such as TomSim (Heuvelink, 1995, 1999). Typically, PBMs include modeling of growth mechanisms (*e.g.*, leaf and crop photosynthesis, light interception, maintenance respiration, biomass production) and the interactions between plants and environmental conditions (*e.g.*, temperature, light, CO_2). A relatively weak component of PBMs is the allocation of assimilates among different organs (leaves, internodes and fruits), which limit their potential application in various environmental scenarios.

More recently, a new generation of plant models, often known as functional-structural plant models (FSPMs), has emerged, which aim to explicitly describe the topology and spatial geometry of plant structure, the interactions among plant structural elements (*e.g.*, shape and orientation of organs), the function of organs (*e.g.*, leaf photosynthesis), the allocation of assimilates among organs, and the feedback between plant growth and development (Vos et al., 2007). To date, FSPMs have been regarded as potential tools for predicting and simulating plant growth and structural development (Renton, 2013), such as with the GreenLab model (de Reffye and Hu, 2003). GreenLab is a generic and mechanistic functional-structural plant model that was developed to simulate plant growth at an organ scale during the organogenesis process. To date, GreenLab has been successfully applied to various species of agricultural crops (Guo et al., 2006; Kang et al., 2012; Qi et al., 2010; Vavitsara et al., 2017); its key advantage over other plant models, which are commonly limited to simulation, is its parametric identification (Christophe et al., 2008). Because of the mathematical formalism of GreenLab, hidden model parameters can be identified using inverse methods from measurement data (Guo et al., 2006; Zhan et al., 2003). Although FSPMs aim to simulate plant-level production in a mechanistic way, the sub-models that simulate a certain process, such as photosynthesis, sometimes take a simplified, empirical approach.

In predicting mass fluxes in the CELSS in previous work, photosynthesis and respiration reactions were modeled based on plant physiology and biochemical reaction knowledge, and the mass balance model for predicting total biomass and CO_2/O_2 concentrations was developed based on stoichiometric equations. However, no humans were involved in the closed system (Hezard et al., 2012; Maclean et al., 2010). Moreover, the developmental stages of plant were absent from the model, and consequently, it is difficult to demonstrate the long-term effects of plant behavior, extending from seedling to mature plant stages, on CO_2/O_2 concentrations.

In this study, we proposed a novel knowledge-and-data-driven modeling (KDDM) approach for simulating plant growth and the dynamics of CO_2/O_2 concentrations in a CELSS that includes plants and humans. This model consists of a 'knowledge-driven (KD)' sub-model and a 'data-driven (DD)' sub-model. The KD sub-model is a combined model of GreenLab and TomSim (GreenLab +). The DD sub-model is a piecewise linear model (PLM) of the CO_2 production and O_2 consumption by the crew member. The two sub-models were integrated through a mass balance model with metabolic stoichiometries, which were derived for CO_2/O_2 concentrations in a closed system. A three-step parameter estimation method was developed to identify the proposed model parameters. Finally, the KDDM approach was evaluated using real data from plant cultivation experiments in a closed system of plants and humans.

2. Materials and methods

2.1. Plant materials and measurements

The data were collected from a two-person, 30-day CELSS integrated test from Nov. 1st to Dec. 1st, 2012 in Beijing, China (Guo et al., 2014b). Lettuce (*Lactuca sativa* L. var. Dasusheng) was planted in the CELSS Integration Test Platform (CITP) of the China Astronaut Research and Training Center, in Beijing, China. The platform was tightly sealed and consisted of such elements as a plant cabin, crew cabin, temperature and humidity control system, plant illumination system, nutrient solution control system, effluent collection and disposal equipment; the volume and area of the CITP was 308 m^3 and 88 m^2, respectively. During the experiment, the cultivation area of the plant was 36 m^2, and the planting density was 56 plants m^{-2}. All of the plants were started from seeds and grew inside the plant cabin for their entire production cycle using a recirculating nutrient hydroponic technique. The Hoagland nutrient solution used nitrate as the sole source of nitrogen. The solution pH was automatically controlled between 6.15 and 6.45 with additions of 1 M nitric acid, and the electrical conductivity (EC) was maintained between 0.195 and 0.205 S m^{-1} with automatic additions of a concentrated stock solution. Light emitting diodes (LED) were used as light sources, which consisted of 90% red light (wavelength 637 nm) and 10% blue light (wavelength 465 nm). The photoperiod was 24 h with photosynthetically active radiation (PAR) of 500 μmol m^{-2} s^{-1} at a distance of 30 cm below the light source. The relative humidity was maintained between 64% and 76%. Water consumption and displacement were monitored and controlled, including water intake, urine, sanitary water, disposed and recycled effluent, and water condensate used for the nutrient solution; the effluent was disposed of and then partly recycled into the nutrient solution, and the condensate water was completely transformed into nutrient solution. The closure of air, water and food in the CITP were at 100%, 90% and 13.9% respectively, with the total material closure at 95.1%. On November 1st, when there were approximately 17 visible leaves, two crew members (male, 32 years, 170 cm, 72.0 kg; male, 38 years, 173 cm, 62.5 kg) entered the crew cabin, which was connected to the plant cabin through ventilation. Beginning on November 24th, a gas balance regulation test was performed (Table 1). The illumination area on the plants was adjusted by turning off a portion of the overhead LED lights to test the gas exchange with less plant photosynthesis.

The collected (hourly average) temporal data included air temperature, atmospheric pressure and CO_2/O_2 concentrations in the atmosphere of the cabin of CITP. During the 30-day experiment, the dry weights of the blades, petioles and stem were measured destructively during five stages along the growing period (Table 2). Furthermore, detailed topological observations were made on six plants twice a week, including the numbers of leaves and phytomer ranks (internode number counting from the base) on the main stem. For a more detailed explanation of the experimental setup of the environmental conditions and the crew members, please refer to Guo et al. (2014b).

Table 1
Setup of the gas balance regulation test.[a]

Duration	Illumination area on the plants
Before test	36 m^2
Day 24–27	24 m^2
Day 27–29	30 m^2
Day 29–30	27 m^2

[a] Each time, the illumination area on the plants was adjusted at 09:00 h by turning off a portion of the overhead LEDs.

Table 2
Dry weight of different types of organs from one harvested plant at each of the five sampling dates.

Sampling date	Dry weights of different types of organs ($g\,m^{-2}$)		
	Blades	Petioles	Stems
Day 5	50.75	11.50	2.75
Day 8	60.00	13.75	6.00
Day 15	84.75	29.00	10.75
Day 22	141.00	37.38	44.75
Day 30	112.75	35.00	61.25

2.2. Models

2.2.1. Knowledge-driven model (GreenLab+)

The GreenLab model was used as the framework for simulating the dynamics of plant organogenesis, biomass production and allocation (de Reffye and Hu, 2003; Kang et al., 2012; Yan et al., 2004). GreenLab obtains source and sink parameters with inverse method, but the biomass production is highly simplified using equations based on the Beer-Lambert Law (Christophe et al., 2008; Guo et al., 2006), considering the environmental conditions in an implicit way. The TomSim model calculates biomass production based on an explicit link to physical plant growth factors (*e.g.*, light, temperature, CO_2), whereas biomass allocation is modeled empirically. To take advantage of both models, the biomass production of GreenLab was replaced with that of the photosynthesis-driven model TomSim. Consequently, a new combined model was developed, called GreenLab+. The framework of GreenLab+ is shown in Fig. 1.

In this work, the time step for calculating crop photosynthesis and maintenance respiration was 1 min. Summing these data provides the daily dry matter production estimate. Biomass allocation and organ expansion were computed daily, with an implicit assumption that plant morphology was stable during a one-day period.

2.2.1.1. Biomass production. Biomass production was simulated using the TomSim model of linking the external conditions (*e.g.*, light, temperature, and CO_2) (Heuvelink, 1995). The daily dry matter (DM) production, dW/dt, is calculated as in Eq. (1):

$$\frac{dW}{dt} = C_f \cdot (P_{gd} - R_m) \tag{1}$$

where dW/dt is the crop growth rate ($g\,DM\,m^{-2}\,d^{-1}$); C_f is the conversion efficiency from assimilates to dry matter ($g\,DM\,g^{-1}\,CH_2O$); P_{gd} is the daily crop gross assimilation rate per unit ground area ($g\,CH_2O\,m^{-2}\,d^{-1}$); and R_m is the daily maintenance respiration rate per unit ground area ($g\,CH_2O\,m^{-2}\,d^{-1}$). More information about P_{gd}, R_m and C_f is provided in Supplementary Material, (a), (b) and (c).

2.2.1.2. Biomass partitioning. In GreenLab+, the assimilate is proportionately distributed to each growing organ according to its sink strength; therefore, the assimilate allocated to an organ of type o appeared at the growth cycle (GC) k, $q_{o,k}$, is calculated as in Eq. (2):

$$\frac{dq_{o,k}}{dt} = \frac{1}{ASR_o} \frac{P_o(\tau(t) - k\gamma)}{D(\tau(t))} P_{gd} \tag{2}$$

where $\tau(t)$ is the thermal time (°Cd) of a plant at time t, that is, $\tau(t) = \int_0^t \max(0, T(s) - T_b) ds$, with a base temperature for lettuce of $T_b = 4\,°C$; γ is a constant and called phyllochron, indicating the thermal time elapsing between successive appearances of phytomers; k (GC) is the observed number of phyllochron of a plant; ASR_o is the assimilate requirement for producing 1 g dry weight of organ o. $D(t)$ is the total demand of all expanding organs at time t, as in Eqs. (3) and (4):

$$D(t) = D_{pg}(t) + N_a(t) S_i \tag{3}$$

$$D_{pg}(t) = \sum_o \sum_{k \in \mathbb{N}} N_o(k) P_o(\tau(t) - k\gamma) \tag{4}$$

where $D_{pg}(t)$ is the primary demand of a plant at plant age t, indicating the sum of the individual organ sink strengths; S_i is the sink of the internode layer for the secondary growth, linked to the thickening of the stem (Table 3); $N_a(t)$ and $N_o(k)$ are the total living number of leaves at age t and the number of organs of type o at growth cycle k, respectively, which were determined by the resulting leaf appearance from detailed topological observations. $P_o(u)$ is the sink strength of the organ type o, which is a function of its thermal age u, as in Eq. (5):

$$P_o(u) = p_o f_{a_o,b_o}(u) \tag{5}$$

where f_{a_o,b_o} is a sink variation function of the organ type o, described by a normalized beta function (Li et al., 2009); p_o is the relative sink strength of the organ type o, indicating the competitive ability of an organ to accumulate biomass, which needs to be estimated as unknown sink parameters (Table 3). Note that the sink strength of blade (p_b) was set to 1 as a reference.

Moreover, the total weight of the given organ o, W_o, can be calculated by summing the biomass of all individual organs of the same type, which is the corresponding data for the measurement, as in Eq. (6):

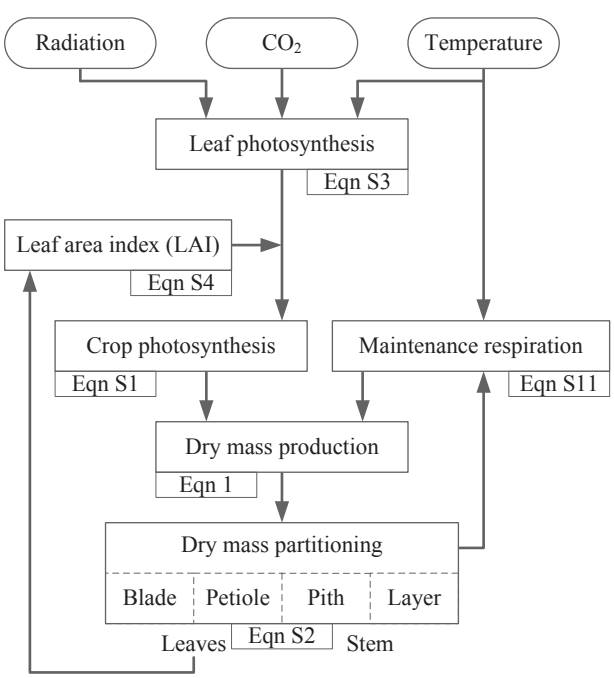

Fig. 1. Framework of GreenLab+ (see Supplementary Material, Eqs. (S1)–(S4) and (S11)).

Table 3
Description of model parameters.

Parameter	Definition	Units
p_p, p_i [a]	Organ sink strength (Eq. (5))	–
S_i	Sink of the internode layer (Eq. (3))	–
$\kappa_{CO_2,S}, \kappa_{CO_2,W}, \kappa_{CO_2,M}, \kappa_{CO_2,P}$ [b]	CO_2 production rate by the crew member (Eq. (9))	$g\,h^{-1}\,person^{-1}$
$\kappa_{O_2,S}, \kappa_{O_2,W}, \kappa_{O_2,M}, \kappa_{O_2,P}$	O_2 consumption rate by the crew member (Eq. (9))	$g\,h^{-1}\,person^{-1}$

[a] p, petiole; i, internode.
[b] S, sleeping; W, normal working; M, morning exercises; P, physical exercises.

$$W_o = \sum_o \sum_k N_o(k) q_{o,k} \tag{6}$$

and the total dry weight (W) is the sum of the dry weights for all of the organs, as in Eq. (7):

$$W = \sum_o W_o \tag{7}$$

GreenLab+ computes the plant growth by simulating the plant process recursively with the principle of the source-sink equilibrium and was thus also called a knowledge-driven model (KDM) (Fan et al., 2015). For the sake of simplicity, GreenLab+ can be rewritten as in Eq. (8):

$$\boldsymbol{y} = \boldsymbol{f}_{\mathrm{k}}(\boldsymbol{x}, \theta_{\mathrm{k}}) \tag{8}$$

where $\boldsymbol{x}$ represents the environmental variables related to plant growth; $\boldsymbol{y}$ denotes the output of GreenLab+; $\boldsymbol{f}_{\mathrm{k}}$ is the function associated with KDM (*i.e.*, GreenLab+); k is the subscript associated with KDM; θ_{k} is a vector of the model parameters, including the organ sink strength (p_{P} and p_{i}) and the sink of the internode layer (S_{i}) controlling plant biomass partitioning, which need to be estimated as the unknown sink parameters (Table 3).

2.2.2. Data-driven model (piecewise linear model)

Human metabolism involves a large number of life-sustaining chemical processes and reactions that occur within a person. The modeling of human metabolism as it relates to CO_2 production and O_2 consumption is a daunting task (Cannon, 2014). However, each person in the crew cabin strictly follows the same work and rest regime every day during the two-person, 30-day CELSS integrated test such that their activities may be divided into four types according to their levels of strength (Table 4). An underlying assumption is made that routine CO_2 production and O_2 consumption by the crew members are stable and identical.

A piecewise linear model (PLM) was developed to represent CO_2 production and O_2 consumption by the crew member, as in Eq. (9):

$$K_{\mathrm{CO_2}} = \sum_{i=\mathrm{S,W,M,P}} n_i \kappa_{\mathrm{CO_2},i}$$
$$K_{\mathrm{O_2}} = \sum_{i=\mathrm{S,W,M,P}} n_i \kappa_{\mathrm{O_2},i} \tag{9}$$

where $K_{\mathrm{CO_2}}$ and $K_{\mathrm{O_2}}$ are the daily CO_2 production and O_2 consumption rates per person, respectively; i is a label of different levels of activities (Sleeping, S; Normal working, W; Morning exercises, M; Physical exercises, P); n_i is the number of hours for the label i (Table 4); and $\kappa_{\mathrm{CO_2},i}$ and $\kappa_{\mathrm{O_2},i}$ are the hourly CO_2 production and O_2 consumption rates for label i per person respectively, which need to be estimated as the unknown respiratory parameters (Table 3).

The PLM was constructed based on the human activity levels rather than the intrinsic metabolic mechanisms, and was thus also called a data-driven model (DDM) (Fan et al., 2015). For the sake of simplicity, PLM can be rewritten as in Eq. (10):

$$\boldsymbol{y} = \boldsymbol{f}_{\mathrm{d}}(\boldsymbol{x}, \theta_{\mathrm{d}}) \tag{10}$$

where d is the subscript associated with DDM (*i.e.*, PLM); $\boldsymbol{y}$ is the output of PLM; θ_{d} is a vector of the model parameters, including CO_2 production and O_2 consumption rates by the crew member, which need to be estimated as the unknown respiratory parameters (Table 3).

Table 4
Work and rest regime of the crew member within the 24 h of each day under different levels of activities (Purser, 2010).

Types	Levels of activity	Activity	Interval[a]	Num. of hours
1	Low level of activity	Sleeping (S)	13–15, 22–24, 0–5	9
2	Light activity	Normal working (W)	8–12, 15–22	11
3	Moderate activity	Morning exercises (M)	5–8	3
4	Heavy activity	Physical exercises (P)	12–13	1

[a] Indicated by hours during a day, from 0 to 24.

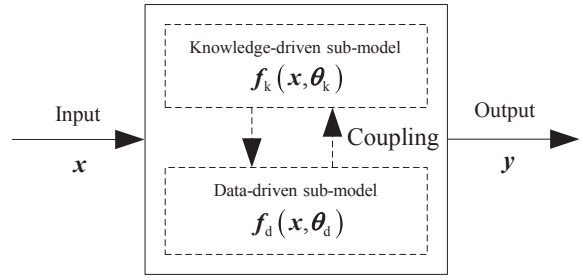

Fig. 2. Schematic diagram of the knowledge-and-data-driven model (KDDM), which primarily consists of the 'knowledge-driven (KD)' sub-model and 'data-driven (DD)' sub-model (Fan et al., 2015).

2.2.3. Knowledge-and-data-driven modeling approach (KDDM)

A knowledge-and-data-driven modeling approach (KDDM) was proposed for simulating both plant growth and the dynamics of CO_2/O_2 concentrations in a CELSS that includes plants and humans. The KDDM primarily consists of two sub-models, as shown schematically in Fig. 2. The upper part of Fig. 2 represents the 'knowledge-driven (KD)' sub-model, which is derived from knowledge of growth mechanisms, including physically based or mechanistic models (*e.g.*, PBMs or FSPMs). The lower part of Fig. 2 represents the 'data-driven (DD)' sub-model, which is constructed solely from data or empirical expressions without using knowledge of intrinsic mechanisms. The material flows of the system is shown in Fig. 3.

In this work, GreenLab+ for biomass production and its partitioning was adopted as the KD sub-model, and PLM was used to CO_2 production and O_2 consumption by the crew member as the DD sub-model. The two sub-models were integrated into the mass balance model with metabolic stoichiometries, which were derived for CO_2/O_2 concentrations in a closed system of plants and humans.

Mass balance model for CO_2/O_2 concentrations. Plant growth and development involve a large number of interconnected processes and reactions. Among these reactions, photosynthesis and respiration reactions affect the production of biomass, as well as the exchange of CO_2/O_2 concentrations between plants and the atmosphere. The reaction scheme can be written as one equation in simple form, as in Eq. (11):

$$\mathrm{CO_2} + \mathrm{H_2O} \overset{\text{light}}{\rightleftharpoons} \mathrm{CH_2O} + \mathrm{O_2} \tag{11}$$

Inspired by the work of Maclean et al. (2010), photosynthesis and respiration reactions in this paper were selected and a mass balance model was proposed for CO_2/O_2 concentrations in a closed system of plants and humans. From the reaction scheme in Eq. (11), the mass

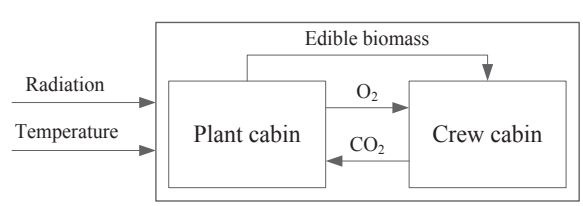

Fig. 3. Material flows of the system [modified from Fig. 2 in Guo et al. (2014b)].

Table 5
Description of the input and output variables for the KDDM approach.

Variable	Definition	Units
T	Temperature	°C
I	Photosynthetically active radiation (PAR)	μmol m^{-2} s^{-1}
C_a	CO_2 concentration in the cabin atmosphere	ppm
O_a	O_2 concentration in the cabin atmosphere	%
W_o	Total dry weights of different types of organs	g m^{-2}

balance model can be written as in Eq. (12):

$$\frac{dC_i}{dt} = \frac{-\frac{44}{30}(P_{gd} - R_m)S_{plant} + \lambda K_{CO_2}}{V_{CITP}}$$
$$\frac{dO_i}{dt} = \frac{\frac{32}{30}(P_{gd} - R_m)S_{plant} - \lambda K_{O_2}}{V_{CITP}} \quad (12)$$

where C_i and O_i are the CO_2 and O_2 concentrations inside the leaves (g m^{-3}), respectively, which are assumed to be approximately equal to their concentrations (C_a and O_a) in the cabin atmosphere; V_{CITP} is the volume of CITP; S_{plant} is the cultivation area of plants; 44/30 and 32/30 are the conversion coefficients from carbohydrates formulated as CH_2O to CO_2 and O_2, respectively, the numerical values representing the molecular weights of CO_2, CH_2O and O_2, respectively; λ is the number of the crew members in the cabin, set to 2; K_{CO_2} and K_{O_2} are the daily CO_2 production and O_2 consumption rates per person, respectively.

For simplicity, the proposed KDDM approach can also be rewritten as in Eq. (13):

$$\boldsymbol{Y} = \boldsymbol{F}(\boldsymbol{X},\Theta) \quad (13)$$

where $\boldsymbol{X}$ and $\boldsymbol{Y}$ are the input and output variables of KDDM, respectively (Table 5); $\boldsymbol{F}$ is the function associated with KDDM; and Θ is a vector of the model parameters (Table 3). The schematic diagram of the KDDM input and output is shown in Fig. 4.

2.3. Parameter estimation

The unknown sink and respiratory parameters (Table 3) were estimated via a generalized least squares (GLS) method, as described in more detail by Zhan et al. (2003) and Guo et al. (2006). The GLS estimator is unbiased, consistent and asymptotically normal. Thus, the model can estimate the model parameters well, even if systematic error and bias exist. However, the fitting of this method is sensitive to the initial value of parameters, so a step-by-step process has been proposed to calibrate the model parameters.

In this paper, a three-step parameter estimation method for KDDM was proposed. In the first step, the closed system was regarded as an open system for plants. The main interest is the plants themselves, T, I and C_a are all regarded as model inputs, and W_o is considered as the model output. The sink parameters (*i.e.*, p_p, p_i and S_i) were identified by the GLS method, whereas other parameters (*i.e.*, $\kappa_{CO_2,S}$, $\kappa_{CO_2,W}$, $\kappa_{CO_2,M}$, $\kappa_{CO_2,P}$, $\kappa_{O_2,S}$, $\kappa_{O_2,W}$, $\kappa_{O_2,M}$, $\kappa_{O_2,P}$) were not considered. The purpose of this stage was to obtain initial values for the sink parameters. In the second step, the sink parameters were fixed as the values obtained from the first stage; then, the remaining respiratory parameters were estimated through the GLS method based on all of the observed data (T and I as model inputs, C_a, O_a and W_o as model outputs). Similar to the first stage, the initial value of respiratory parameters could be obtained. In the final step, the estimated values from the above two stages were regarded as the initial values of the sink and respiratory parameters; next, all of the observed data were used to obtain the optimal parameter values using the GLS method. For each of the three steps, the weighted least square error was minimized by searching for the best parameter values, $J_\Omega(\Theta)$, given by Eq. (14):

$$J_\Omega(\Theta) = [\hat{\boldsymbol{Y}} - \boldsymbol{F}(\boldsymbol{X},\Theta)]^T \Omega [\hat{\boldsymbol{Y}} - \boldsymbol{F}(\boldsymbol{X},\Theta)] \quad (14)$$

where $\hat{\boldsymbol{Y}}$ is the observed target data for fitting; Ω is a diagonal positive matrix, which is calculated from the variance of the data. Advantages of this method include its rapid convergence.

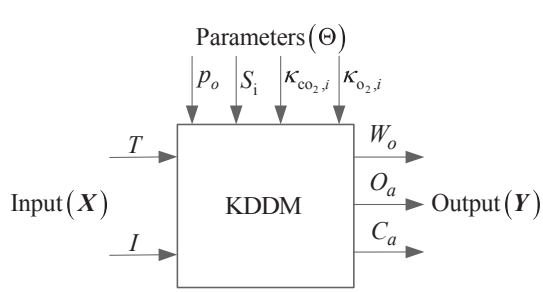

Fig. 4. Inputs and outputs of the KDDM approach for modeling plant growth processes and the dynamics of CO_2/O_2 concentrations in the CELSS (see Tables 3 and 5 for definitions of the symbols).

2.4. Model verification

The data from the two-person, 30-day CELSS integrated experiment were divided into training and testing sets, including the dry weights of different types of organs from five sampling dates and hourly average CO_2/O_2 concentrations. The data from the first 24 days were retained as the training set, and the remaining data (the last 6 days) were used as the testing set. This finding is reasonable because the regulation test was performed on the 24th day (Table 1). Therefore, the model parameters can be identified on the training data set using the above three-step parameter estimation method; then, the identified model was verified on the testing data set, which was not used for identification of the model parameters. Model computation and model fitting on the experimental data were conducted using the open-source GreenScilab software (http://www.greenlab.org.cn/cPlant/software_greenscilab.html).

3. Results

3.1. Experimental results

Hourly average temperatures, atmospheric pressure, CO_2 and O_2 concentrations during the 30-day experiment (from 09:00 h, November 1st) are shown in Figs. 5 and 6. The ranges in temperature and atmospheric pressure were from 25.13 to 25.65 °C and from 100.45 to 103.28 kPa, respectively, which indicates that temperature and atmospheric pressure exhibited very little variation. Instead, CO_2 concentrations show high variation, ranging from 261.25 to 1925.5 ppm. The O_2 concentrations varied from 21.054 to 21.386%.

As shown in Fig. 6, the air exchange balance was built soon after the crew members entered the cabin. During each day, the CO_2 and O_2 concentrations exhibited a similar pattern: the CO_2 concentration rose

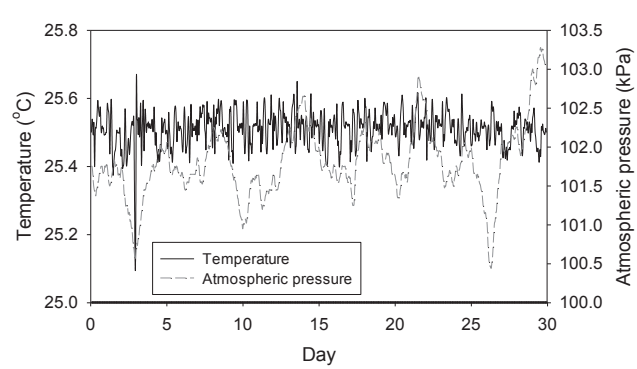

Fig. 5. Hourly average temperature and atmospheric pressure during the 30-day experiment.

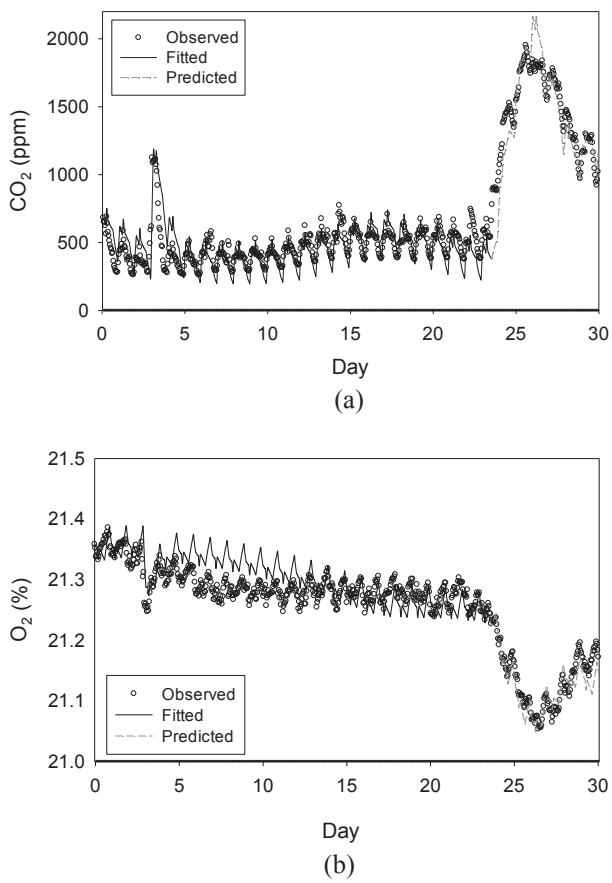

Fig. 6. Observed, fitted and predicted values of CO_2 and O_2 concentrations over time. (a) CO_2; (b) O_2.

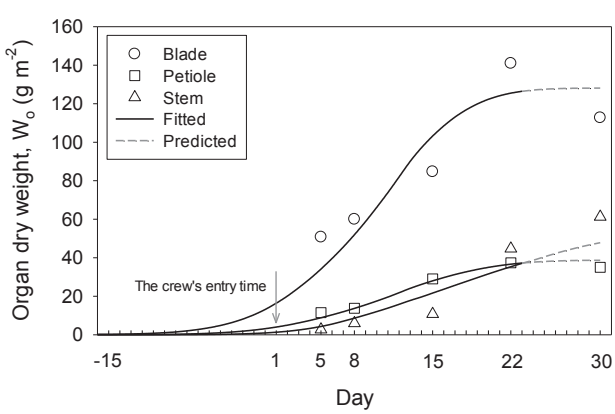

Fig. 7. Dry weights of three different types of organs (blades, petioles and stems), showing the observed, fitted and predicted organ biomass over time.

during the day when the crew members were doing daily activities, reaching maximum value at approximately 13:00 h because of the physical exercise, and dropped in the night when the crew members was sleeping. The trend in O_2 concentration was the opposite, indicating good correspondence with CO_2 concentration. Note that there were approximately 20 abnormal data points for CO_2/O_2 concentrations between Day 3 and Day 4 that were caused by a sudden power failure. On the 24th day, the gas balance was broken as the regulation test started featuring decreasing plant illumination area (Table 1); the CO_2 concentration rose quickly when the illumination area on the plants was regulated to 24 m^2 and gradually decreased after the plant illumination area was regulated to 30 m^2; finally, it fluctuated within a small range from an illumination area of 27 m^2 on the 30th day (Fig. 6).

Table 6
RMSE and R between the predictions and observations for the dry weights of different types of organs from five sampling dates, and the hourly average CO_2 and O_2 concentration from 30 days.

	CO_2 concentration (ppm)	O_2 concentration (%)	Dry weights of different types of organs ($g\,m^{-2}$)		
			Blades	Petioles	Stems
RMSE[a]	122.44	0.03	15.23	2.11	9.92
R[b]	0.96	0.94	0.92	0.99	0.97

[a] RMSE, root mean square error.
[b] R, Pearson correlation coefficient.

Furthermore, the dry weights of the three different types of organs from five different sampling dates are shown in Fig. 7. The blade is the main compartment in the weight as lettuce is a leafy plant.

3.2. Estimated model parameter values

Following the three-step parameter estimation method mentioned above, the target data from the training data set, including the dry weights of different types of organs from the first four sampling dates, the hourly average CO_2 and O_2 concentrations from the first 24 days, were fitted simultaneously. Their fitting curves are shown in Figs. 6 and 7. The root mean square error (RMSE) and Pearson correlation coefficient (R) between the predictions and observations of the dry weights of different types of organs from five sampling dates, and the hourly average CO_2/O_2 concentrations from 30 days, are provided in Table 6. The optimal parameter values estimated by the proposed method and their reference values are listed in Table 7. The reference values for an average, healthy 70 kg adult are provided (Brake and Bates, 1999; Kannan, 2015). Based on the respiratory parameters, the daily CO_2 production and O_2 consumption of the crew member was calculated in Eq. (9) as follows: $K_{CO_2} = 1167.01\ g\,d^{-1}\,person^{-1}$ and $K_{O_2} = 859.95\ g\,d^{-1}\,person^{-1}$, respectively, which are close to the reference values (approximately 1000 and 840 $g\,d^{-1}\,person^{-1}$, respectively) according to previous studies (Taylor, 2015).

3.3. Predicted results of the biomass, CO_2 and O_2 concentrations

Using the estimated parameter values, the plant biomass, CO_2 and O_2 concentrations were computed for the last 6 days, with less plant illumination area. The CO_2 concentration was augmented soon after the illumination area dropped to 24 m^2 from Day 24 to 27 because of reduced CO_2 absorption by the plants and increased plant respiration. The trend became inverse after Day 27, as the illumination area increased to

Table 7
Estimated parameter values from the training data set, including the dry weights of different types of organs from the first four sampling dates, and the hourly average CO_2 and O_2 concentrations from the first 24 days.

Parameter	Estimated values	Reference values (Brake and Bates, 1999; Kannan, 2015)	Units
p_p, p_i, S_i	0.243, 0.310, 0.925	–	–
$\kappa_{CO_2,S}$	38.92	< 47.45	$g\,h^{-1}\,person^{-1}$
$\kappa_{CO_2,W}$	47.40	~47.45	$g\,h^{-1}\,person^{-1}$
$\kappa_{CO_2,M}$	71.44	~61.68	$g\,h^{-1}\,person^{-1}$
$\kappa_{CO_2,P}$	81.01	> 61.68	$g\,h^{-1}\,person^{-1}$
$\kappa_{O_2,S}$	19.05	< 42.90	$g\,h^{-1}\,person^{-1}$
$\kappa_{O_2,W}$	41.95	~42.90	$g\,h^{-1}\,person^{-1}$
$\kappa_{O_2,M}$	53.34	~55.77	$g\,h^{-1}\,person^{-1}$
$\kappa_{O_2,P}$	67.06	> 55.77	$g\,h^{-1}\,person^{-1}$

See Table 3 for the definitions of the parameters. Note: p_b was set to 1 as a reference.

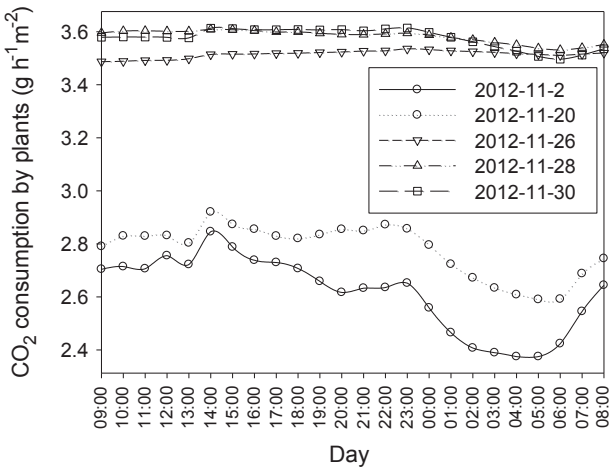

Fig. 8. Computed (net) CO_2 consumption by plants within a 24-h day.

30 m^2. Beginning on Day 29, the illumination area on the plants dropped to 27 m^2. Encouragingly, the model predicted well the above result for the three stages (Figs. 6 and 7), which indicates that the model system, once calibrated, is capable of being extended to new environmental condition.

3.4. Computed CO_2 consumption and O_2 production by plants

According to the estimated values of sink and respiratory parameters, the results of (net) CO_2 consumption and O_2 production by plants were inferred by model calculation, rather than by direct measurement. The five most informative curves of hourly computed (net) CO_2 consumption by plants are shown in Fig. 8. The results indicate that hourly computed (net) CO_2 consumption by plants varied with the CO_2 concentration of the system, with planting areas of 36 m^2 that increased as plants grew and the leaf area increased (curves Day 2 and Day 20). During the last six days (from Day 24 to 30), the plant (net) CO_2 consumption by unit area remained stable, regardless of high hourly vibrations of CO_2 concentrations. This was because the CO_2 concentration of the system became high and the leaf area index (LAI) reached a high value, exceeding 6, meaning that both the leaf and canopy photosynthesis were saturated according to Eqs. (2) and (7). Overall, the hourly computed (net) CO_2 consumption of plants in the curves for 5 days varied between 2.4 and 3.6 $g\,h^{-1}\,m^{-2}$, and the CO_2 absorbing ability of plants was higher during the day than at night, especially in the first 24 days.

Furthermore, GreenLab+ not only computes the (net) CO_2 consumption and O_2 production by plants but also their corresponding components: CO_2 consumption and O_2 production through photosynthesis (*i.e.*, P_{gd}, Eq. (S1) in the Supplementary Material), and CO_2 production and O_2 consumption through respiration (*i.e.*, R_m, Eq. (S11) in the Supplementary Material). The curve of daily computed (net) CO_2 consumption by plants, which consisted of CO_2 consumption through photosynthesis and CO_2 production through respiration, are shown in Fig. 9. It is clear that the CO_2 production by plants through respiration is very low compared to the CO_2 consumption.

In this work, we assumed that O_2 is released in a one-to-one molar ratio with the absorption of CO_2. That is, for each kg of CO_2 absorbed, 32/44 kg of O_2 is produced, and the numerical values representing the molecular weights of O_2 and CO_2, respectively. Therefore, the computed (net) O_2 production by plants and their components (*i.e.*, O_2 production through photosynthesis and O_2 consumption through respiration) are not listed here.

3.5. Computed CO_2 production and O_2 consumption by the crew member

The CO_2 production and O_2 consumption by the crew member per day are expressed by their corresponding respiratory parameters (Eq. (9)), but once the parameters of GreenLab+ were obtained, the daily data could be derived reversely from the observed CO_2 and O_2 data according to Eq. (12), as shown in Fig. 10 (curves for 5 days are given). Overall, the CO_2 production and O_2 consumption by the crew member per day changed based on the work and rest regime within 24 h for different levels of activities, and the ranges of their values are given in Table 8.

Moreover, CO_2 production and O_2 consumption by the crew member (*i.e.*, $\widehat{K}_{CO_2}$ and $\widehat{K}_{O_2}$) per day can be calculated by summing the computed CO_2 production and O_2 consumption of the crew member within 24 h, as shown in Fig. 11. The average values of $\widehat{K}_{CO_2}$ and $\widehat{K}_{O_2}$ over 30 days are as follows: 1178.53 $g\,d^{-1}\,person^{-1}$ (Std. = 62.60, CV = 5.31%) and 867.54 $g\,d^{-1}\,person^{-1}$ (Std. = 47.26, CV = 5.45%), respectively.

3.6. Gas balance and limit state in the CITP

The amount of CO_2 change per day in the CITP was derived directly from the observed CO_2/O_2 concentrations, whereas the daily amounts of CO_2 production by the two crew members and (net) CO_2 consumption by all plants were inferred from the model calculation (Fig. 12). The results indicate that their daily amounts remain relatively stable during quite a long period (Day 5–23), which means that a balance of gas exchange between plants and humans was established. Specifically, when the power in the CITP was temporarily disrupted (between Day 3 and Day 4) or the new illumination policy on the plants was performed (since Day 24), the balance was severely disturbed; however, once power was restored or the illumination area on the plants was regulated to 27 m^2, the new balance was rebuilt again due to photosynthesis.

In a steady-state, *i.e.*, $dC_i/dt = 0$, according to Eq. (12), the CO_2 concentration (C_a) in the cabin can be computed according to the planting area (S_{plant}) and the number of the crew members (λ), *i.e.*, $P_{net} = \lambda\ K_{CO2}/S_{plant} = 2 \times 1167.01/36 = 64.83\ g\,CO_2\,d^{-1}\,m^{-2}$. This computation provides a steady-state CO_2 concentration; that is, $C_a = h^{-1}(P_{net}) = 572.5$ ppm, where h^{-1} is an inverse function of f, and f is a function of net photosynthesis (P_{net}) versus the leaf internal CO_2 concentration (C_i), expressed by the photosynthesis-driven model TomSim (see Section 2.2.1). On the other hand, if the question of interest is 'how much planting area is needed to maintain a balance?' the limited planting area is computable and thus can be used for providing guidance for experimental design. According to the maximum photosynthetic rate, *i.e.*, $P_{net} = 44/30\ (P_{gd} - R_m) = 86.64\ g\,CO_2\,d^{-1}\,m^{-2}$, the minimal planting area to maintain the CO_2 balance is 26.91 m^2 ($S_{plant} = \lambda\ K_{CO2}/P_{net} = 2 \times 1167.01/86.64 = 26.94\ m^2$, Eq. (12)) for the two crew members.

4. Discussion

4.1. Benefits of the KDDM approach

Generally, predicting mass fluxes in a human-plant system require the following: (1) plant photosynthesis, biomass allocation, leaf area and respiration must be properly simulated; (2) a module describing CO_2 emissions and O_2 absorption by humans is necessary; and (3) a mass-balance model of the interested variable and the model must be identifiable. The aim of this study was to develop a KDDM approach for simulating plant growth and the dynamic of CO_2/O_2 concentrations in a CELSS of plants and humans by integrating mechanistic and empirical models. Although previous studies (Hezard et al., 2012; Maclean et al., 2010) have proposed a simple mass balance model for predicting total biomass and CO_2/O_2 concentrations, the developmental stage of plants was absent, and no humans were involved in a closed system. In our

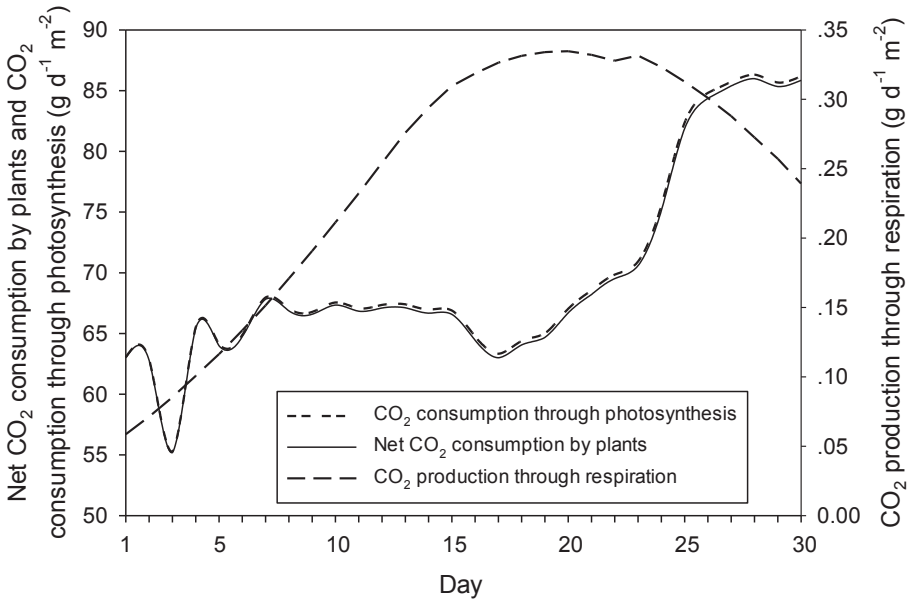

Fig. 9. Computed (net) CO_2 consumption by plants, which consisted of CO_2 consumption through photosynthesis and CO_2 production through respiration.

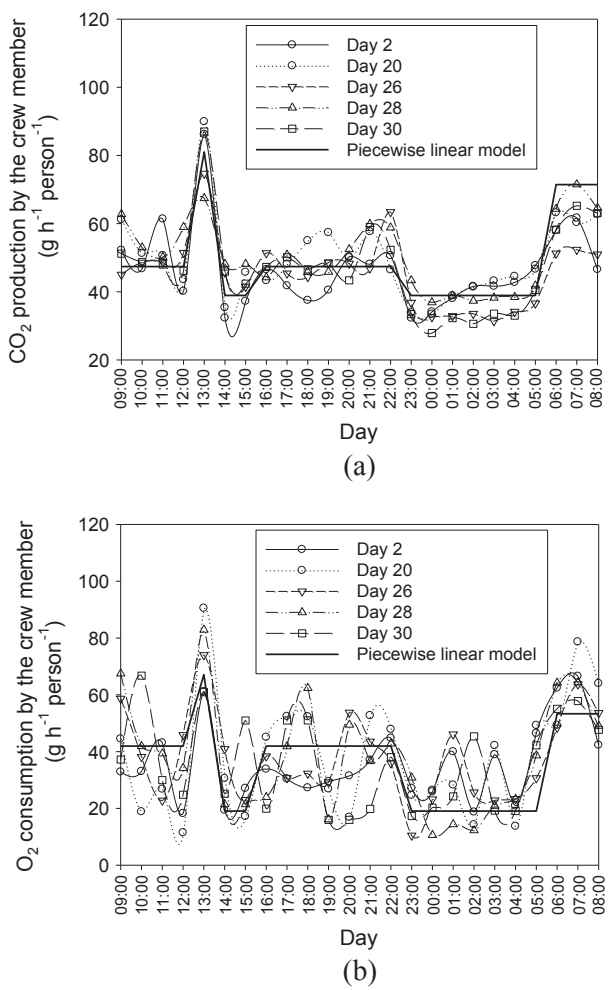

Fig. 10. Computed CO_2 production and O_2 consumption by the crew member within a 24-h day. (a) CO_2; (b) O_2.

study, multiple variables (the dry weight of different types of organs, and hourly CO_2/O_2 concentrations) of the closed human-plant system have been fitted well simultaneously, as explained and predicted by the proposed KDDM approach. Moreover, the model explains well the interaction among the crew members, plants and environment and provides deeper understanding of the behaviors of the closed system. Furthermore, the model unveiled several underlying state variables in the CITP that are difficult to measure, including the hourly and daily CO_2 production and O_2 consumption by the crew member, the hourly and daily CO_2 consumption (photosynthesis) and production (respiration) by plants.

Table 8
Ranges of CO_2 production and O_2 consumption by the crew member under different levels of activity, which were inversely derived from the observed CO_2 and O_2 concentrations based on the KDDM approach.

Levels of activity	Activity	CO_2 production $\kappa_{CO_2,i}$[a] ($g\,h^{-1}$ $person^{-1}$)	O_2 consumption $\kappa_{O_2,i}$[a] ($g\,h^{-1}$ $person^{-1}$)
Low level of activity	Sleeping (S)	27.88–48.14	10.44–50.97
Light activity	Normal working (W)	37.48–63.40	11.44–67.44
Moderate activity	Morning exercises (M)	46.54–71.46	42.28–78.62
Heavy activity	Physical exercises (P)	67.42–89.89	60.96–90.47

[a] $\kappa_{CO_2,i}$ and $\kappa_{O_2,i}$ are the hourly CO_2 production and O_2 consumption rates of the label i per person, respectively.

The advantage of the KD sub-model (GreenLab +) is that it carefully takes into account knowledge regarding plant development and growth such that the plant respiration and biomass growth are simultaneously simulated as two sub-processes of the same object. Moreover, GreenLab + combines the advantages of two plant models: the organ-level biomass partitioning and the inverse estimation of sink parameters of the GreenLab model, and the biomass production of the TomSim model. As a result, once calibrated, the model not only computed the CO_2 level in the cabin but also gave the underlying story of CO_2 absorption and emissions by plants (Fig. 8). The contribution of plants to the closed system was then clearly quantified without using sophisticated instruments (Fig. 12).

The DD sub-model (PLM) for simulating hourly human CO_2 production overwhelmed the difficulty of the modeling of the complex human metabolic process by regarding it as a black box. Once calibrated, the KDDM provided an estimation of human respiration data

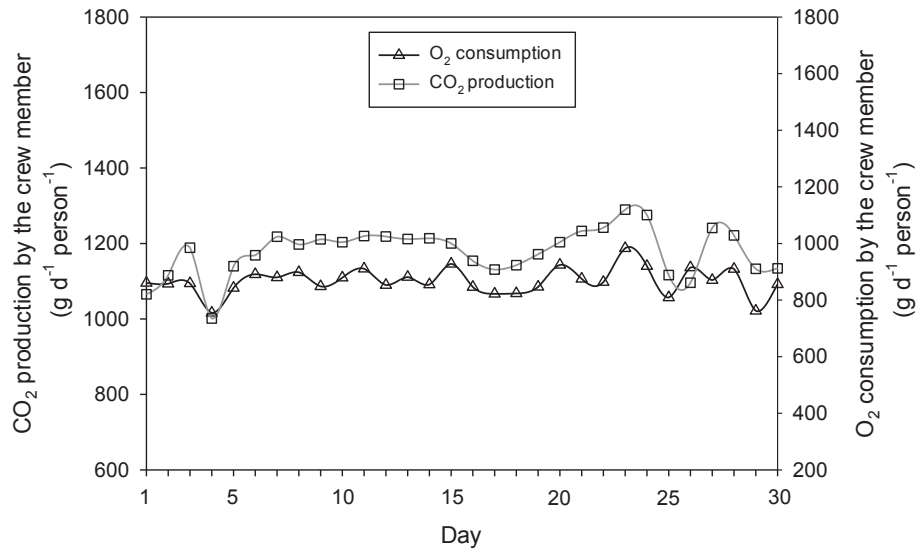

Fig. 11. Computed CO_2 production and O_2 consumption by the crew member every day for 30 days.

(Fig. 10). The estimated values of the respiratory parameters of the crew member were basically in accordance with the above reference values (Table 7). The daily CO_2 production and O_2 consumption per person (1167.01 g and 859.95 g were nearly the same as the average results (1178.53 g and 867.54 g) that were inversely derived from observations with the KDDM approach (Fig. 11). However, our results (K_{CO_2} = 1167.01 g d^{-1} person^{-1} and K_{O_2} = 859.95 g d^{-1} person^{-1}) were higher compared with the two-person, 3-day crew member metabolism test results (843.0 g d^{-1} person^{-1} and 755.0 g d^{-1} person^{-1}) in Guo et al. (2014b), which could be due to the effects of measuring plant growth in the plant cabin.

4.2. Plasticity and contribution of plants in the closed system

Over the long term, plants are expected to provide oxygen, food and water for the crew members in a closed system. As a biological component of the system, plants play the role of an automatic regulator of CO_2 concentrations in the cabin. The gas phase in the cabin is carefully modulated by the plants. Specifically, when the power in the CITP was temporarily disrupted, the CO_2 increased significantly, but once the power was restored, the CO_2 concentration dropped due to photosynthesis, thus emphasizing the importance of plants in regulating gas composition. Moreover, plants adapt to the environment as needed. Even during one day, the plants change their photosynthetic rate according to whether the crew members are sleeping or doing exercise (Fig. 8).

A steady CO_2 level can be maintained over a long period (from Day 5 to 23, Fig. 6) when there are no external factors. A balance of CO_2 supply and demand was maintained (Fig. 12) because of the existence of plants. Since all of the CO_2 consumption is from plants, as long as the other environmental factors are not limiting, the steady-state CO_2 concentration could be computed (572.5 ppm). These results coincide with observed data, as shown in Fig. 6a. Such results are helpful in the design of the CELSS or experimental setup. However, there is a limit to the moderate ability of plants to reach a balance. On Day 24, when the illumination area on the plants dropped to 24 m^2, which is below the limiting area of 26.91 m^2, the CO_2 level increased rapidly as the plants were not sufficient to absorb more CO_2, even if the plants increased their photosynthetic ability (Fig. 8). When the illumination area on the plants increased to 30 m^2 on Day 27, a new balance began to be achieved (Figs. 6 and 9). Next, when the illumination area on the plants was set to 27 m^2 on Day 29, the gas balance could still be maintained.

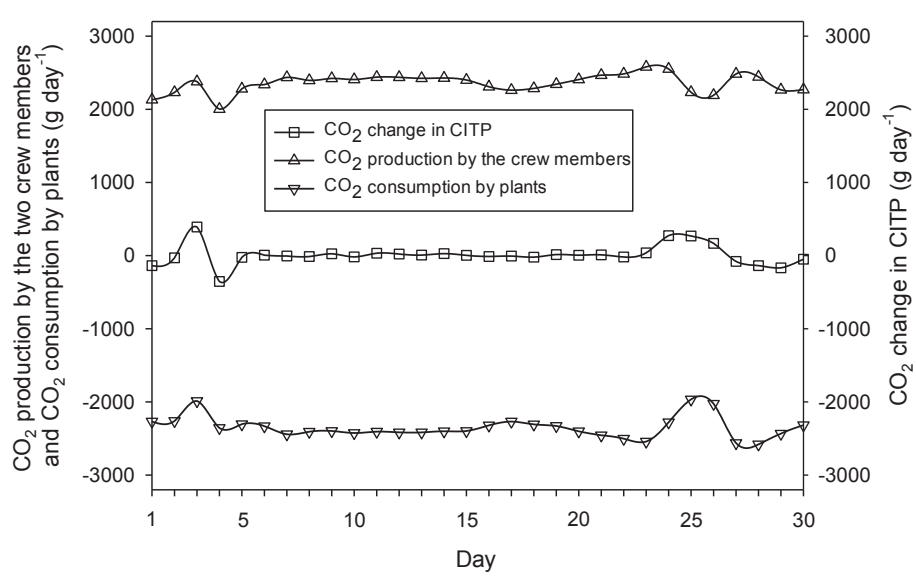

Fig. 12. Carbon dioxide change in the CITP caused by CO_2 production of the two crew members and CO_2 consumption of plants.

Furthermore, the computational results suggest that at least 13.47 m^2 of plants could supply O_2 for one human, which is consistent with previous findings (20–25 m^2) (Guo et al., 2014b; Wheeler, 2015; Wheeler and Sager, 2006). Using the computational approach, the suitable planting area could be computed, which is useful for arranging the plant schedule in the CELSS.

Compared to plants grown in an open or half-open system, such as a glasshouse, the behaviors of plants in the closed system are completely different. The total CO_2 absorption by the plants is stable, whereas the total plant biomass (Fig. 7) and the leaf area index (data not shown) increased. This is because the limiting factor is CO_2 availability, which is dependent on the crew members. Nevertheless, this model helps to provide a better understanding of how to increase crop production in a glasshouse by regulating multiple environmental factors simultaneously, including the CO_2 level, light intensity, and humidity.

4.3. CO_2 production and O_2 consumption by the crew member

Generally, CO_2 production and O_2 consumption by the crew member vary from one person to another, depending on the body composition, age and gender. Modeling CO_2 production and O_2 consumption by the crew member on a daily basis is one of the important challenges. In this work, a simplified assumption was made that the crew members strictly follow the same work and rest regime within a 24-h day, that consists of four different levels of activities (Table 4). This was reasonable as there was a strict schedule and set training. That is, the changing laws of CO_2 production and O_2 consumption by the crew member each day was assumed to be identical (Eqs. (9), (12)). Based on this assumption, the KDDM approach described the data fairly well (Figs. 6 and 7), which indicates that this simplifying assumption is valid and useful. The results derived from the KDDM approach (Table 7 and Fig. 10) further confirm the validity and usefulness of the assumption.

5. Conclusions

This paper presents a knowledge-and-data-driven modeling (KDDM) approach for simulating plant growth and the dynamics of CO_2/O_2 concentrations in a closed ecological life support system of plants and humans by integrating mechanistic and empirical models. The results of the application of the KDDM approach to a two-person, 30-day integrated CELSS test reveal that the proposed KDDM approach not only provides accurate computation of both the dry weights of different plant compartments and CO_2/O_2 concentrations but also quantifies the underlying material flows among the crew members, plants and environment. Furthermore, the present study provides a promising advance regarding plant growth modeling using GreenLab+. A new version, which can be called KDDM_GreenLab+, is able to take advantage of the data-driven model while maintaining the physically based model as the core component.

Although the simulation results are promising, there are still several limitations to our approach that need to be studied in future work. First, the KDDM approach should be evaluated in another separate data set with different people/plants and experiments. Second, a more detailed approach will be needed in which the model is expanded to include other key processes of plant growth, such as leaf transpiration and root water uptake, especially if one considers edible food and drinkable water from plants. Since the system is highly electricity-costly, a next step is to study how to adjust the illumination policy while maintaining sufficient O_2 levels for humans. Furthermore, the system behavior is influenced by the crop type; thus, it is worth studying how other (fruity) plants behave in such a system, as leafy plants are not sufficient to provide a full diet for humans. Finally, the current work can be a starting point for further optimization of cabin design and experimental setup of CELSS (*e.g.*, environmental control, planting schedule). This method can even be further extended and developed as a generic tool for the use in a half-closed system, such as a glasshouse.

Acknowledgements

This work was supported in part by the Chinese Manned Space Engineering Advance Research Projects (Grant number: Y5W2021), the National Science Foundation of China (Grant numbers: 61573348, 31400623, 31700315) and the Doctor Start-up Foundation of Chongqing University of Posts and Telecommunications (Grant number: E010A2017023). Special thanks to research assistant Lifeng Qin for his support in the experimental set-up. We are grateful to the anonymous reviewers and editors for their comments on this manuscript.

Appendix A. Supplementary material

Supplementary data associated with this article can be found, in the online version, at http://dx.doi.org/10.1016/j.compag.2018.03.006.

References

Brake, D., Bates, G., 1999. Criteria for the design of emergency refuge stations for an underground metal mine. J. AusIMM 304, 1–8.
Cannon, W.R., 2014. Concepts, challenges, and successes in modeling thermodynamics of metabolism. Front. Bioeng. Biotechnol. 2, 53.
Christophe, A., Letort, V., Hummel, I., Cournède, P.-H., de Reffye, P., Lecœur, J., 2008. A model-based analysis of the dynamics of carbon balance at the whole-plant level in Arabidopsis thaliana. Funct. Plant Biol. 35, 1147–1162.
Diao, J., De Reffye, P., Lei, X., Guo, H., Letort, V., 2012. Simulation of the topological development of young eucalyptus using a stochastic model and sampling measurement strategy. Comput. Electron. Agric. 80, 105–114.
de Reffye, P., Hu, B.-G., 2003. Relevant qualitative and quantitative choices for building an efficient dynamic plant growth model: GreenLab case. In: Hu, B.-G., Jaeger, M. (Eds.), International Symposium on Plant Growth Modeling, Simulation, Visualization and Their Applications-PMA'03. Springer and Tsinghua University Press, Beijing, China, pp. 87–107.
Fan, X.-R., Kang, M.-Z., Heuvelink, E., de Reffye, P., Hu, B.-G., 2015. A knowledge-and-data-driven modeling approach for simulating plant growth: a case study on tomato growth. Ecol. Model. 312, 363–373.
Finetto, C., Rapisarda, A., Renzoni, D., Sabbagh, A., Sinesi, C., 2008. Food and Revitalization Module (FARM) for Moon Human Exploration. SAE Technical Paper.
Guo, S., Ai, W., Tang, Y., Cheng, Q., Shen, Y., Qin, L., Ma, J., Zhu, J., Ren, J., 2014a. Study on O_2 generation and CO_2 absorption capability of four co-cultured salad plants in an enclosed system. Adv. Space Res. 53, 1551–1556.
Guo, S., Dong, W., Ai, W., Feng, H., Tang, Y., Huang, Z., Shen, Y., Ren, J., Qin, L., Zeng, G., 2014b. Research on regulating technique of material flow for 2-person and 30-day integrated CELSS test. Acta Astronaut. 100, 140–146.
Guo, S., Tang, Y., Zhu, J., Wang, X., Yin, Y., Feng, H., Ai, W., Liu, X., Qin, L., 2008. Development of a CELSS experimental facility. Adv. Space Res. 41, 725–729.
Guo, Y., Ma, Y., Zhan, Z., Li, B., Dingkuhn, M., Luquet, D., De Reffye, P., 2006. Parameter optimization and field validation of the functional–structural model GREENLAB for maize. Ann. Bot. 97, 217–230.
Heuvelink, E., 1995. Dry matter production in a tomato crop: measurements and simulation. Ann. Bot. 75, 369–379.
Heuvelink, E., 1999. Evaluation of a dynamic simulation model for tomato crop growth and development. Ann. Bot. 83, 413–422.
Hezard, P., Dussap, C.-G., Sasidharan, L,S., 2012. Higher plant modelling for life support applications: first results of a simple mechanistic model. In: 39th COSPAR Scientific Assembly, p. 758.
Kang, M.-Z., Heuvelink, E., Carvalho, S.M., De Reffye, P., 2012. A virtual plant that responds to the environment like a real one: the case for chrysanthemum. New Phytol. 195, 384–395.
Kannan, R., 2015. Breathing rates and breathing air constituents. J. Innov. Sci., Eng. Technol. 2, 557–558.
Li, Z., Le Chevalier, V., Cournede, P.-H., 2009. Towards a continuous approach of functional-structural plant growth. In: Fourcaud, T., Zhang, X.-P. (Eds.), The Third International Symposium on Plant Growth Modeling, Simulation, Visualization and Applications (PMA'06). IEEE Computer Society, Beijing, China, pp. 334–340.
Maclean, H., Dochain, D., Waters, G., Dixon, M., Chaerle, L., Van Der Straeten, D., 2010. Identification of simple mass balance models for plant growth-Towards food production on manned space missions. IFAC Proc. 43, 335–340.
Purser, D.A., 2010. Asphyxiant components of fire effluents. In: Hull, R., Stec, A. (Eds.), Fire Toxicity. Woodhead Publishing Ltd., Cambridge, UK, pp. 118–198.
Qi, R., Ma, Y., Hu, B.-G., de Reffye, P., Cournède, P.-H., 2010. Optimization of source-sink dynamics in plant growth for ideotype breeding: a case study on maize. Comput. Electron. Agric. 71, 96–105.
Renton, M., 2013. Aristotle and adding an evolutionary perspective to models of plant architecture in changing environments. Front. Plant Sci. 4, 1–4.
Taylor, E.R., 2015. Human deep-space travel and colonization: technical issues. New Space 3, 154–164.
Vavitsara, M.E., Sabatier, S., Kang, M., Ranarijaona, H.L.T., de Reffye, P., 2017. Yield analysis as a function of stochastic plant architecture: Case of *Spilanthes acmella* in the wet and dry season. Comput. Electron. Agric. 138, 105–116.

Vos, J., Evers, J.B., Buck-Sorlin, G., Andrieu, B., Chelle, M., De Visser, P.H., 2009. Functional–structural plant modelling: a new versatile tool in crop science. J. Exp. Bot. 61, 2101–2115.
Vos, J., Marcelis, L., De Visser, P., Struik, P., Evers, J., 2007. Functional-structural plant modelling in crop production: adding a dimension. In: Vos, J., Marcelis, L., de Visser, P., Struik, P., Evers, J. (Eds.), Functional-Structural Plant Modelling in Crop Production. Springer (Wageningen UR Frontis Series), Wageningen, The Netherlands, pp. 1–12.
Wheeler, R.M., 2015. NASA's controlled environment agriculture testing for space habitats. New Space 3, 154–164.
Wheeler, R.M., Sager, J.C., 2006. Crop production for advanced life support systems. NASA Technical Reports. Paper 1.
Yan, H.-P., Kang, M.-Z., De Reffye, P., Dingkuhn, M., 2004. A dynamic, architectural plant model simulating resource-dependent growth. Ann. Bot. 93, 591–602.
Yin, X., Struik, P.C., 2016. Crop systems biology: where are we and where to go? In: Yin, X., Struik, P. (Eds.), Crop Systems Biology. Springer International Publishing, pp. 219–227.
Zhan, Z.-G., De Reffye, P., Houllier, F., Hu, B.-G., 2003. Fitting a functional-structural growth model with plant architectural data. In: Hu, B.-G., Jaeger, M. (Eds.), International Symposium on Plant Growth Modeling, Simulation, Visualization and Their Applications-PMA'03. Springer and Tsinghua University Press Beijing, China, pp. 108–117.